Reliability of Power Modules in Hybrid Vehicles

Conference Paper · April 2009

3 authors:

Andre Christmann
Infineon Technologies
29 PUBLICATIONS **41** CITATIONS

SEE PROFILE

M. Thoben
University of Applied Science and Arts Dortmund
81 PUBLICATIONS **631** CITATIONS

SEE PROFILE

Krzysztof Mainka
Infineon Technologies
5 PUBLICATIONS **160** CITATIONS

SEE PROFILE

Some of the authors of this publication are also working on these related projects:

Project   Reliability of Power Modules View project

Reliability of Power Modules in Hybrid Vehicles

André Christmann, Infineon Technologies AG, Max-Planck-Straße 5, D-59581 Warstein, Germany
Markus Thoben, Infineon Technologies AG, Max-Planck-Straße 5, D-59581 Warstein, Germany
Krzysztof Mainka, Infineon Technologies AG, Max-Planck-Straße 5, D-59581 Warstein, Germany

Abstract

The life time of a component is defined by the reliability demands place on it due to its operating environment and operation conditions. To evaluate the necessarily thermal / power cycle stability of a power semiconductor module in a hybrid electrical vehicle (HEV), a vehicle driving cycle profile is used to calculate the thermal reliability requirements. The calculations are based on power loss calculation, thermal modeling and a general approach of a life cycle model. This paper discusses the reliability requirements due to active and passive thermal stress on various joints such as solder or bond joints resulting by using different connections of a power module to varied cooling systems.

1.   Introduction

HEV typically combines a combustion engine with an electrical drive train. To develop a system with variable speed a HEV is equipped with power semiconductors typically packaged in a module. Nowadays most of the commercial vehicles use more or less conventional power modules mounted on an air cooler or a separated liquid cooling system. Hybrid systems of different car manufacturer are so dissimilar that a comparison between them is rather impossible. Beside the cooling systems also the packaging and even the silicon differs.

To make such systems more comparable the presented investigations are based on a common "basis-power module" called HybridPACK that is adapted to different cooling systems. For a considered configuration a common set of input parameters such as drive cycle, type of the electrical motor and even the electrical characteristics of the semiconductors are used. Of course, influences due to different driving strategies are neglected for simplification.

In power electronics the component temperature and temperature changes have major influences on the reliability. Therefore, a procedure was developed, which computes the temperature over the whole driving cycle. The calculations are based on power loss calculation and thermal modeling.

These calculations between the thermal conductivity from the module through to the cooler, the active thermal stress on various joints such as solder or bond joints can be evaluated. By transforming the thermal stress into reliability test data a prediction of lifetime is possible.

For judging whether the basic type module HybridPACK is appropriate for a given application (cooling, driving conditions etc.) some exemplary results of reliability tests are given.

2.   From drive cycle to reliability test

2.1.   Reliability tests

During the life time a module is exposed to passive temperature swings coming from the environment (climate) and active temperature cycles generated by operation. Temperature cycling and power cycling tests represent these conditions.

Temperature Cycling: In temperature cycling tests the temperature of a power module is changed by variation of the ambient temperature (TST: Thermal Shock Test) or the temperature of the case (TC: Thermal Cycle Test) without electrical stressing. This test is applied mainly to evaluate the lifetime of the solder joints and to evaluate the resistance to the sudden changes in temperature the device can experience during storage, transportation or in use.

Power Cycling: Power cycling (PC) tests are used to determine the resistance of a semiconductor device to thermal and mechanical stresses due to cycling the power dissipation of the internal semiconductor die and internal connectors. This happens when load currents are periodically applied and removed causing rapid changes of temperature. The power cycling test is representative to high temperature operating life [1].

The predominant failure mechanisms due to thermal stress are the degradation of solder layers (solder fatigue) and the bond wire lift-off.

2.2. General approach

Fig. 1 explains the procedure how the representing number of test cycles for a reliability test can be derived from the information of the inverter system (cooling conditions) and the driving strategy (mission profile, motor and drive control) for a given set of electrical parameters (electrical characteristics of the power module). Only the few red marked parameters were varied during this investigation.
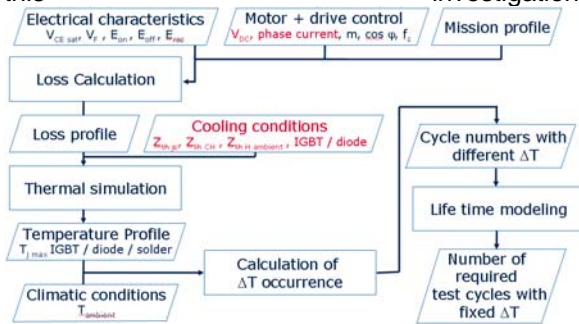
Fig. 1. General approach for calculating the number of equivalent tests cycles. Only the parameters marked red were varied in investigation

2.3. Basic Conditions (Input parameter)

In order to get independent from drive conditions, motor characteristics as well as chip characteristics a common set of input parameters was chosen.

A well known and investigated power semiconductor module was selected. This module type is designed for Mild Hybrid Electrical Vehicle applications for a power range up to 20 kW [2]. Designed for a junction operation temperature at 150°C, the module accommodates a Six-Pack configuration and is rated up to 400A/600V (Fig. 2).

The mission profile was developed by using a drive cycle which represents more or less a typical vehicle cycle including several start stop sequences and 5 ten second long recuperation cycles under full load.

Module gate driving conditions was assumed ideal although this may lead to an underestimation of power losses in the complete inverter system. This fact was compensated by calculating the power losses for the worst case conditions (maximum temperature) during an incremental step [6].

Fig. 2. The basic module is based on the HybridPACK™1 [3][4][5]

2.4. Calculation of power losses

The power losses of a module result by adding the static (P_{DC}: conducting) and the dynamic (P_{SW}: switching) losses.

The power losses calculation in the dies for inverter operation use sinusoidal half-waves to model the heat in the dies. This approach is based on the calculation methods used in IPOSIM [7].

Based on this approach the conducting losses of the IGBT³ [8] and the diode can be calculated based on the electrical parameters of the module [9] [10].

$$P_{IGBT\_DC} = \frac{I^2 r}{8} + \frac{I \cdot V_{CE0}}{2\pi} + m \cdot \cos(\varphi) \cdot \left(\frac{I^2 r}{3\pi} + \frac{I \cdot V_{CE0}}{8} \right) \quad [1]$$

$$P_{Diode\_DC} = \frac{I^2 r_D}{8} + \frac{I \cdot V_{F0}}{2\pi} - m \cdot \cos(\varphi) \cdot \left(\frac{I^2 r_D}{3\pi} + \frac{I \cdot V_{F0}}{8} \right) \quad [2]$$

It has to be mentioned that the parameters r, V_{CE0}, r_D and V_{F0} are temperature T dependent.

The switching losses of a power module can be described by using equation 3 and 4. The losses are determined by the product of the switching frequency f_{sw} and the switching energies E_{on_nom}, E_{off_nom}, E_{rec_nom} at nominal conditions (V_{nom}, I_{nom}, T_{nom}) adapted to the applied voltage V_{DC}, current $\hat{i}$ and temperature T_j [11].

$$P_{IGBT\_SW} = \frac{f_{sw}}{\pi} \cdot \left(E_{on\_nom} + E_{off\_nom} \right) \cdot \frac{\hat{i}}{I_{nom}} \cdot \frac{V_{DC}}{V_{nom}} \cdot \left(\frac{T_J}{T_{nom}} \right)^{\alpha} \quad [3]$$

$$P_{Diode\_SW} = \frac{f_{sw}}{\pi} \cdot E_{rec\_nom} \cdot \left(\frac{\hat{i}}{I_{nom}} \right)^{\kappa} \cdot \frac{V_{DC}}{V_{nom}} \cdot \left(\frac{T_J}{T_{nom}} \right)^{\alpha} \quad [4]$$

All necessary parameters can be extracted from the power module datasheet [12].

2.5. Thermal model

For calculating the power module reliability, it is necessary to know transient temperatures of semiconductor junctions, as well the system solder temperature. The solder joint temperature is necessary for the calculation of the solder fatigue due the thermal cycling.

The thermal model, describing the dependency between the dies virtual junction temperatures (T_{vj}), system solder average temperature (T_{sold}) and the power losses of IGBT (I) and Diode (D), is given in a transient thermal impedance matrix form with following equation:

$$\begin{pmatrix} T_{vj(I)}(t) \\ T_{vj(D)}(t) \\ T_{(Sold)}(t) \end{pmatrix} = \begin{pmatrix} Z_{th,ja(I)}(t) & Z_{th(D \to I)}(t) \\ Z_{th(I \to D)}(t) & Z_{th,ja(D)}(t) \\ Z_{th(I \to Sold)}(t) & Z_{th(D \to Sold)}(t) \end{pmatrix} \cdot \begin{pmatrix} p_I(t) \\ p_D(t) \end{pmatrix} + \begin{pmatrix} T_{Amb} \\ T_{Amb} \\ T_{Amb} \end{pmatrix} \quad [5]$$

The model included apart from the transient thermal impedance junction-to-ambient ($Z_{th,ja}$) of IGBT and Diode, also cross coupling elements which describe the interdependencies between the chips and the solder. Therefore power losses of the silicon leads to an increase of the temperature in the solder layer [6].

An equivalent circuit representation of the equation 5, implemented into circuit simulator, is shown in Fig. 3.
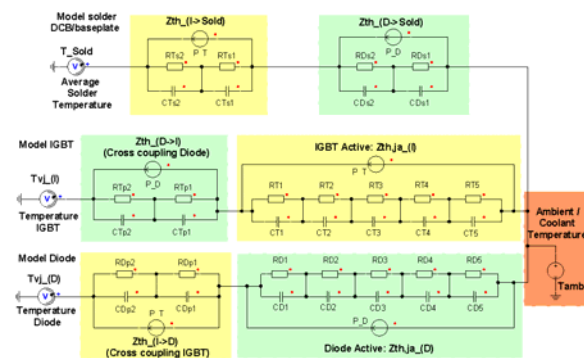
Fig. 3. RC-network (Foster-model)

For transient thermal impedance entries approximation the Foster RC-networks was chosen [13]. The values of the R's and C's were derived by 3D transient finite element simulation using the system's material properties and physical dimensions or they were extracted from measurement.

2.6. Temperature profile simulation

With the aid of the thermal model the temperature of the IGBT, the diode and the solder can be calculated for the load conditions of a given driving cycle.

Hereby the conditions of the applications were taken into account, e. g. for an air cooled system which is mounted nearby the passenger compartment the ambient temperature was set to 40°C (Fig. 4).
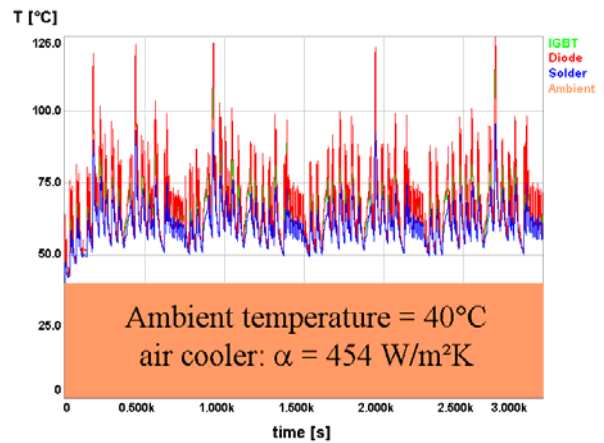
Fig. 4. Temperature profile of a power module mounted on air cooler for one 3000 second driving cycle

In this case the resulting maximum temperatures were $T_{j\,max\,IGBT}$ = 118°C, $T_{j\,max\,diode}$ = 126°C and $T_{j\,max\,solder}$ = 96°C respectively (see also Table 2).

The temperature itself is not the major parameter which is responsible for solder and bond wire aging but rather the temperature swings. Therefore an automatic algorithm is implemented in the simulation to extract the temperature differences ΔT.

2.7. Determination of ΔT occurrence

Active cycles: Fig. 5 shows the number of occurrence for a certain temperature swing at the diode for an air cooled system. Temperature ranges below 3 K are neglected since they do not decrease lifetime significant. Most of the swings lead to an increase of temperature below 30°K. Only a few cycles with higher ΔT occurred. 5 high temperature swings was observed at ΔT > 60°K. These swings represent the peaks of Fig. 4. Overlaid to these active swings are always passive swings due to the operational environmental.

Passive cycles: The heating up of a cooling system during operation also leads to a temperature swing which has to be considered during life time calculation.
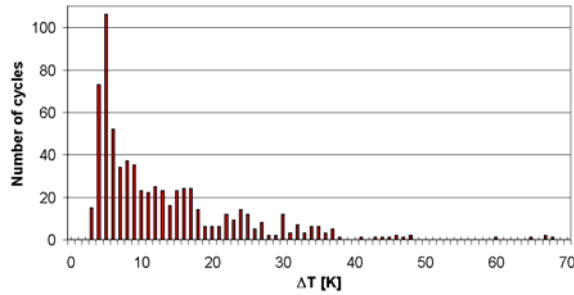
Fig. 5. Diode: Number of cycles for different ΔT (α=454W/m² K) for one driving cycle

Assuming a vehicle lifetime of 15 years and two cycles per day 10950 additionally cycles are applied to a power module. The environmental temperature was defined in table 1 reaching from 5 days with -25°C up to 35 days with 30°C outdoor temperature.

Outdoor temperature	-25	-20	-15	-10	-5	0	5	10	15	20	25	30	sum
Days per year	5	10	10	20	25	30	45	50	50	50	35	35	
Cycles per day	2	2	2	2	22	2	2	2	2	2	2	2	
Cycles per year	10	20	20	40	50	660	90	100	100	100	70	70	
Cycles in 15 years	150	300	300	600	750	900	1350	1500	1500	1500	1050	1050	10950

Table 1. Passive temperature swings due to heating up the cooling system from environmental temperature to operation temperature

The temperature swing of the heating up sequence was always defined as the difference between the maximum temperature during the driving cycle and the minimum temperature at the start equal to the environmental temperature (see Table 3).

A reliability test applying different temperature swings to a device is rather nonpractical. Therefore standardization to a common ΔT has to be done.

3. Transformation from duty cycles to test cycles

3.1. Solder joint acceleration calculation

Models for mechanical failure, material fatigue or material deformation typically have terms relating to stress cycles or change in temperatures. A model of this type known as the (modified) Coffin-Manson model has been used successfully to model crack growth in solder and other metals due to repeated temperature cycling as equipment is turned on and off. The form of this frequently-cited equation makes it clear that fatigue will result in much earlier failure when the joint

experiences wider temperature excursions. The most useful derivative of this equation is probably the relationship between the number of cycles to failure with two different thermal ranges (ΔT_{duty_cycle} and ΔT_{test}) [14]. Although different exponents have been mentioned in the literature, the calculations that have been done use an exponent of 3,3. This model takes the form

$$\frac{n_{duty\_cycle}}{n_{test\_cycle}} = \left(\frac{\Delta T_{test\_cycle}}{\Delta T_{duty\_cycle}} \right)^{[2\text{ - }4,5]} \quad [5]$$

The equivalent number of test cycles n_{test_cycle} for a specified test temperature range ΔT_{test} can be calculated from the number n_{duty_cycle} of duty cycles with a given ΔT_{duty_cycle} coming from the temperature profile.

3.2. Wire bond acceleration calculation

The relation between an arbitrary parameter set under duty condition (current I, junction temperature T_j, operation time t_{on} and temperature swing ΔT) and the number of equivalent cycles for a known reliability test setup is given in equation 6.

$$\frac{n_{test\_cycle}}{n_{duty\_cycle}} = \frac{\Delta T_{test}^{-4.416} \cdot e^{\frac{1285}{T_{j\min}+273}} \cdot t_{on,test}^{-0.463} \cdot I_{test}^{-0.716}}{\Delta T_{duty}^{-4.416} \cdot e^{\frac{1285}{T_{j\min,duty}+273}} \cdot t_{on,duty}^{-0.463} \cdot I_{duty}^{-0.716}} \quad [6]$$

This formula also contains the ratio of the different temperature differences but it has been modified due to results of a large number of performed tests [15].

Based on equation 6 the number of equivalent test cycles (conditions: ΔT_{test}=100K, $T_{j,min}$=50°C, $t_{on, test}$ = 2s and reference current of I_{test} = 400A) results from the summation of all p transformation for any duty cycle i calculated in chapter 2.5.

$$n_{test,sum} = \sum_{i=1}^{p} n_{test,i} = \sum_{i=1}^{p} n_i \frac{100^{-4.416} \cdot e^{\frac{1285}{50+273}} \cdot 2^{-0.463} \cdot 400^{-0.716}}{\Delta T_{j,i}^{-4.416} \cdot e^{\frac{1285}{Ti+273}} \cdot t_{on,i}^{-0.463} \cdot I_i^{-0.716}} \quad [5]$$

4. Variation of parameters

4.1. Cooling conditions

Cooling capability: 2 air cooled systems, 1 liquid cooled system and 1 direct cooled system were compared.

For the air and the liquid cooled system thermal grease between the flat baseplate and the flat cooler was supposed.

The difference cooling capabilities of these two systems were taken into account by using different heat transfer coefficient a applied to the back side of the heat sink. (See Table 2: a = 124 W/m²K - poor air cooler; a = 454 W/m²K - forced air cooler; a = 20000 W/m²K - strong liquid cooler).

	cooling efficiency	electrical parameters		maximum temperature			
	α_{eff} [W/m²K]	V_{DC} [V]	I_{rms} [A]	Ambient [°C]	IGBT [°C]	Diode [°C]	Solder [°C]
air cooler	124	150	150	40	150	157	128
air cooler forced	454	150	150	40	118	126	96
air cooler forced	454	300	80	40	94	100	79
liquid cooler	20000	150	150	70	124	129	97
liquid cooler	20000	150	150	95	149	154	122
direct cooling PinFin	10 l / min	150	150	70	100	107	85
direct cooling PinFin	10 l / min	300	80	70	90	95	80
direct cooling PinFin	10 l / min	150	150	95	128	135	111

Table 2. Variation of system parameters

In order to get an ideal heat transfer from the module to the cooler a PIN FIN structured baseplate was assumed. This module type is directly mounted on an open liquid cooler with direct contact of the pins and the cooling medium. Therefore the thermal grease with it's bad thermal conductivity can be removed. Due to the direct contact of the baseplate to the liquid the value α is not defined. In such a case the flow rate of liquid represents different cooling capabilities.
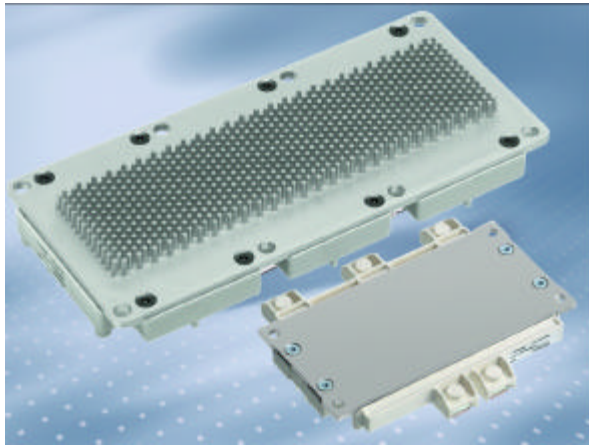
Fig. 6. Example of a PIN FIN structured baseplate (HybridPACK^{TM}2) [16][17] in comparison to a flat baseplate

Ambient temperature: As mentioned in chapter 2.6 the maximum ambient temperature was set to 40°C for an air cooled system and it was defined to 70°C/95°C for the liquid cooled systems (Table 2).

4.2. Electrical parameters

Battery voltage: A lot of car manufacturer prefer to apply relative low voltages for the high voltage battery of a mild hybrid system. Higher voltage can only be realized by adding further cells to the battery what clearly leads to higher cost and weight. In order to get a feeling how the system is influenced by the battery voltage V_{DC} two set of electrical parameters were compared (Table 2).

5. Results

As shown in Fig. 1 the active swings generated during the drive cycle and the passive swings due to the operational environmental have to be considered. For the silicon side the worst case condition of IGBT and diode has to be considered. Due to the 5 recuperation cycles the highest load is on the diode. Therefore most of the examples represent the diode.

Power Cycling: For the failure mechanism bond wire lift off the maximum temperature of the bond wire is set to the maximum chip temperature $T_{j\ max}$. The life cycle modeling allows the number of equivalent power cycles for passive and active cycles to be calculated.

The equivalent number of active cycles was calculated by transforming the number of ΔT occurrence given in Fig. 5 by using equation 7. Similar to the passive case the number of driving cycles was set to 10950.

For calculating the equivalent number of test cycles for the stress due to passive cycles the transformation of the cycle numbers from Table 1 was done. The result is shown is Table 3.

Outdoor temperature	-25	-20	-15	-10	-5	0	5	10	15	20	25	30	sum
Days per year	5	10	10	20	25	30	45	50	50	50	35	35	
Cycles per day	2	2	2	2	2	22	2	2	2	2	2	2	
Cycles per year	10	20	20	40	50	660	90	100	100	100	70	70	
Cycles in 15 years	150	300	300	600	750	900	1350	1500	1500	1500	1050	1050	10950
Minimum Chip Temperature [°C]	-25	-20	-15	-10	-5	0	5	10	15	20	25	30	
Maximum Chip Temperature [°C]	126	126	126	126	126	126	126	126	126	126	126	126	
ΔT chip [K]	151	146	141	136	131	126	121	116	111	106	101	96	
equivalent number of cycles ΔT=100K	293	521	462	814	893	936	1220	1170	1004	855	506	424	9097

Table 3. Power cycling diode: Calculation of equivalent test cycles representing the passive temperature swings

Thermal Cycling: A similar procedure was applied while transforming passive and active cycles as described in chapter 3.1. Maximum temperature for the solder was derived from the drive cycle calculation (Fig. 4).

Outdoor temperature	-25	-20	-15	-10	-5	0	5	10	15	20	25	30	sum
Days per year	5	10	10	20	25	30	45	50	50	50	35	35	
Cycles per day	2	2	2	2	2	22	2	2	2	2	2	2	
Cycles per year	10	20	20	40	50	660	90	100	100	100	70	70	
Cycles in 15 years	150	300	300	600	750	900	1350	1500	1500	1500	1050	1050	10950
Minimum Chip Temperature [°C]	-25	-20	-15	-10	-5	0	5	10	15	20	25	30	
Maximum Chip Temperature [°C]	126	126	126	126	126	126	126	126	126	126	126	126	
ΔT chip [K]	151	146	141	136	131	126	121	116	111	106	101	96	
equivalent number of cycles ΔT=100K	293	521	462	814	893	936	1220	1170	1004	855	506	424	9097

Table 4: Thermal cycling solder: Calculation of equivalent test cycles representing the passive temperature swings

5.1. Overview

Fig. 7 and Fig. 8 show a comparison of equivalent test cycles for the different parameters.

Power cycling: In Fig. 7 the number of equivalent test cycles (conditions: ΔT_{test}=100K, $T_{j,\,test}$=150°C, $t_{on,\,test}$ = 2s and reference current of I_{test} = 400A) for a power cycling test is given as the sum of cycles generated by active operation and the number of cycles representing the passive swings.
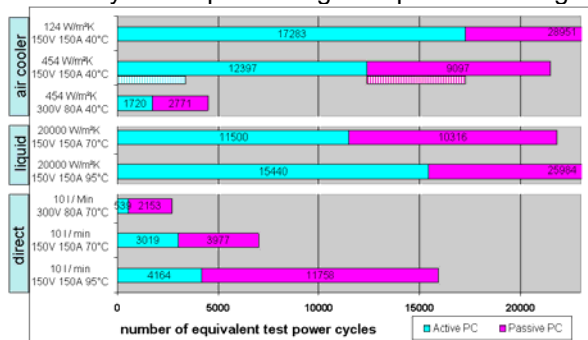
Fig. 7. Number of equivalent power cycles for different parameters for a given drive cycle

Thermal cycling: In Fig. 8 the number of equivalent test cycles (conditions: $\Delta T = 80K$) for a thermal cycling test are given as the sum of cycles generated by active operation and the number of cycles representing the passive swings.
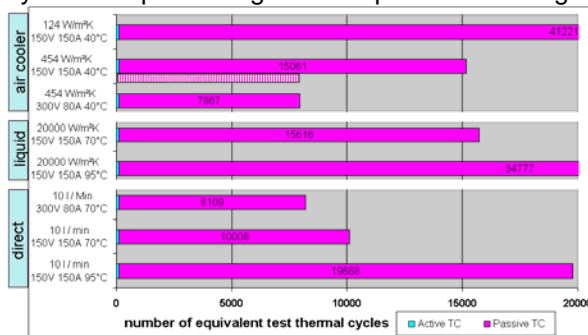
Fig. 8. Number of equivalent thermal cycles for different parameters for a given drive cycle

The influence of the active cycles can be neglected in every case. This is justified because of the very low temperature swing of the solder during operation (< 55°C; forced air cooler) compared to the high ΔT of the passive swings.

5.2. Statements

Even the two reliability tests can not be compared although the trend for both test are similar. This is because in both cases a higher ΔT leads to a higher number of equivalent test cycles.

1) A better cooling capability leads to lower reliability requirements.

(Of course, such a trivial statement can be given by everyone – the aim of this paper is to give a hint how much the cooling capability influences the reliability requirements.)

2) A forced air cooler with ambient temperature of 40°C has similar performance as a liquid cooled module with ambient temperature of 70°C.

3) Increase of coolant temperature from 70°C to 95°C doubles the number of equivalent cycles. The use of a separate (independent) cooling circuit for the inverter seems to be mandatory. The use of the engine cooling cycle with temperature up to 125°C can not be realized with conventional mounting and joining techniques.

4) Even without module operation the solder suffers from temperature swings due to changes in the outdoor temperature.

5) The use of a direct cooled module reduce significant the demands on module.

6) Increase of the battery voltage reduces the power cycling requirements of the air cooled system by a factor of 4; thermal requirements are reduce by 40%.

7) The influence of the bus voltage is reduced by the use of better cooling capability.

8) The avoiding of the 5 ten second long recuperation cycles under full load reduces the requirements by 60% for power cycling and 40% for thermal cycling (compare dashed columns in Fig. 7 and Fig. 8 for forced air cooler).

The last two statements express the necessity for a global system approach for a HEV development by adjusting the driving strategy, the cooling system, the battery voltage and the module thermal load cycles stability. A joint development between vehicle manufacturer, the inverter supplier and the supplier of the power semiconductor module avoids an over sizing of the power module and cost can be reduced.

5.3. Experimental results

For judging whether a module is appropriate for a given application (cooling, driving conditions etc.) the thermal load cycles stability of the power module has to be known. The lifetime of the module can then be derived by using results of reliability tests. For our basic type module HybridPACK[TM]1 (see Fig. 2 and Fig. 6) some tests were performed.

For the different parameter set ups shown in Fig. 7 only the case of the very poor air cooler (α = 124W/m²K) and the use of a hot liquid coolant (95°C) while mounting the module with thermal grease lead to equivalent number of cycles exceeding the power cycling capability of a state of the art bonding process.

Under the conditions valid for Fig. 8 (ΔT = 80K, $T_{j\,min}$ = 25°C) only a small (<10 %) delamination was observed after 20000 cycles and no increase of the thermal resistance R_{th} (which is used as failure criteria) was measured. Even 25000 cycles were reached in this test with still being in the required limits.
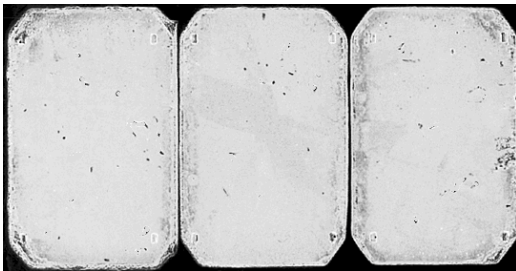
Fig. 9. Ultrasonic measurement of the delamination after 20000 cycles (ΔT = 80K)

The picture shows that even by using a copper base plate it is possible to reach numbers of cycles which were so far reserved to material stacks using AlSiC base plates.

Similar improvements were made with the increase of thermal load cycle stability of the system soldering for thermal shock tests (TST) with high ΔT.
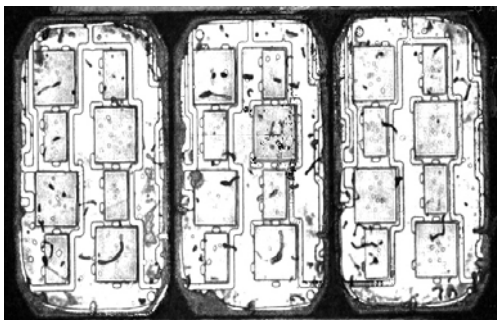
Fig. 10. Ultrasonic measurement of the delamination after 1000 cycles [-40°C –150°C]

Due to the fact that the delamination occurs at the edge of the ceramic substrates the thermal resistance of the silicon chips is not affected.

6. Conclusion

Nowadays most of the commercial hybrid vehicles use more or less conventional power modules. Due to a missing standardization hybrid systems of different car manufacturer are so dissimilar that a comparison between them is rather impossible. In order to make inverter systems more comparable the presented investigations were based on a unified "basis-power module" and a common set of input parameters.

To evaluate the necessarily thermal / power cycle stability of a power semiconductor module in a hybrid electrical vehicle (HEV), a procedure was developed, which computes the temperature of the silicon and the solder over a given driving cycle.

By transforming the thermal stress on solder and bond joints due to active and passive thermal stress into reliability test data a calculation of equivalent test cycles was done.

In this paper eight different sets of parameter varying in cooling conditions and/or battery voltage were compared. One result was that a joint development between vehicle manufacturer, the inverter supplier and the supplier of the power semiconductor module is very helpful in finding a cost effective solution by adjusting the driving strategy, the cooling system, the battery voltage and the module thermal capabilities.

7. Remark

Some remaining correlation of variables used in the model restricts the model to ranges of test conditions of selected data. Therefore, authors strongly recommend not applying the model without consulting experts at Infineon Technologies. Furthermore some of the showed tests results may differ to results of released products due to unmentioned changes in material or processes.

8. Literature

[1] IEC 60749-34, Ed. 1.0, 2004-03; IEC60747-9, 1998

[2] Graf, I.: Reliable IGBT Power Semiconductor Modules for Hybrid Electrical Vehicles, Bodo´s Power, 08-07, p. 22-24, 2008.

[3] Münzer, M.; Thoben, M.; Christmann, A.; Vetter, A.; Specht, B.: Halbleiter für das „grüne" Auto, Elektronik Praxis, 2007

[4] Münzer, M.; Thoben, M.; Vetter, A.; Christmann, A.; Ferber, G.: Suitability of Power Semiconductor Modules for HEV Applications, Automotive Power Electronics, 2006

[5] www.infineon.com/hybridpack

[6] Thoben, M. et al.: From vehicle drive cycle to reliability testing of Power Modules for hybrid vehicle inverter, PCIM Europe 2008, Nuremberg, 2008.

[7] IPOSIM: IGBT Power Simulation Tool available at www.infineon.com

[8] Kanschat, P.; Rüthing, H.; Umbach, F.; Hille, F.: 600V-IGBT³: A detailed Analysis of Outstanding Static and Dynamic Properties, PCIM Europe 2004, Nuremberg, 2004.

[9] Srajber, D.; Lukasch, W.: The calculation of the power dissipation for the IGBT and the inverse diode in circuits with the sinusoidal output voltage, electronica conference, 1992.

[10] Schütze, T.: IPOSIM, a Flexible Selection and Calculation Tool, Power Systems Design, December 2005.

[11] Mainka, K.; Aurich, J.; Hornkamp, M.: Fast and reliable average IGBT simulation model with heat transfer emphasis, PCIM Europe 2006, Nuremberg, 2006.

[12] Datasheet FS400R06A1E3, www.infineon.com

[13] Lutz, J.: Halbleiter-Leistungsbauelemente, Springer-Verlag, 2006.

[14] Karya, Y.; Otsuka, M.: Mechanical fatigue characteristics of SnAgX solder alloys, Journal of Electronic materials, volume 27-11, p. 1229-1235, 1998.

[15] Bayerer, R. et al.: Model for Power Cycling lifetime of IGBT Modules – various factors influencing lifetime, CIPS 2008, Nuremberg, March 2008.

[16] Münzer, M.; Thoben, M.; Christmann, A.; Vetter, A.; Specht, B.: Application Focused Power Semiconductor Module Design for Hybrid Electric Vehicles, Power Electronics Europe, Issue 2, 2007

[17] Volke, A.; Bo, Z.; Christmann, A.; Schlörke, R.: Reliable IGBT Modules for (Hybrid) Electric Vehicles, PCIM, China, 2007